Single and Double Hole Quantum Dots in Strained Ge/SiGe quantum wells

Will J. Hardy, C. Thomas Harris, Yi-Hsin Su, Yen Chuang, Jonathan Moussa,
Leon N. Maurer, Jiun-Yun Li, Tzu-Ming Lu and Dwight R. Luhman

Nanotechnology 30 (2019), 215202

Motivation

- Silicon as a leading contender for hosting spin-based qubits
  - Long coherence times, isotropic enrichment, CMOS processing
  - Si/SiGe heterostructures with low disorder interface
  - Material related issues, e.g large variation of the valley splitting (35 – 270 μeV) [1]

- Ge/SiGe heterostructures
  - Holes as dominant charge carriers -> p-type orbital characters, suppresses qubit decoherence via hyperfine
  - Large heavy-hole and light-hole band splitting (up to 100 meV) -> results from confinement and strain [2]
  - Heavy-hole ground state has no degenerate states
  - EDSR possible due to large cubic Rashba spin-orbit coupling strength -> simplified device design
  - Large g-factor (up to $g \sim 28$)

- In this paper
  - Single and double quantum dots in planar Ge/SiGe using a single layer gate layout
  - Hole effective mass of $m^* \sim 0{,}08\ m_0$

[1] Borselli et al., APL 98, 123118 (2011)
[2] Moriya et al., PRL 113, 086601 (2014)

Device and Heterostructure

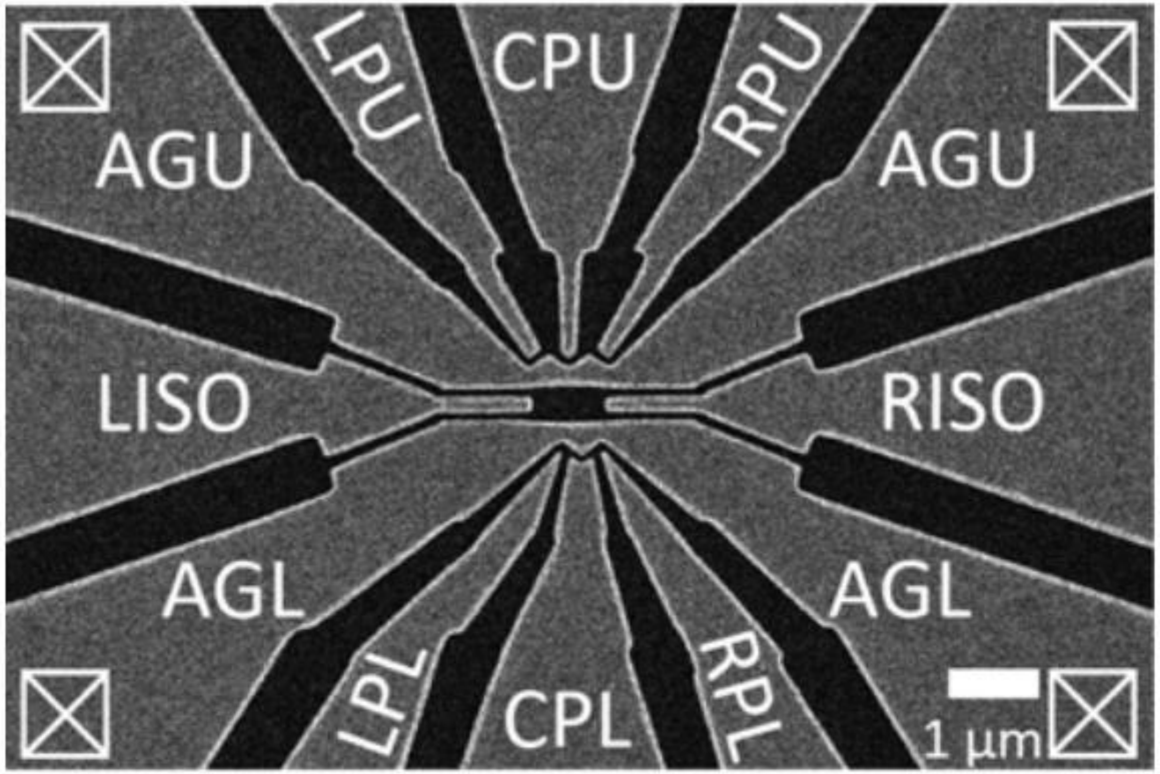

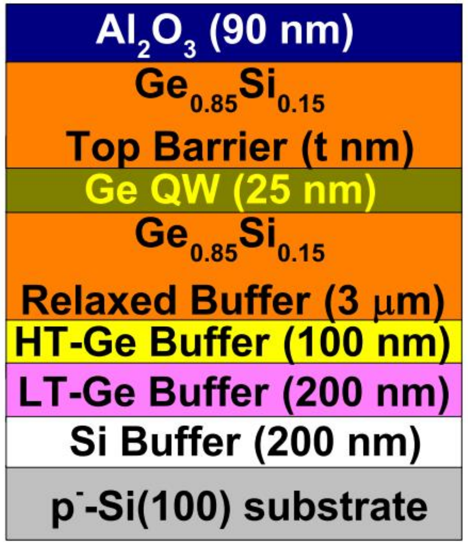

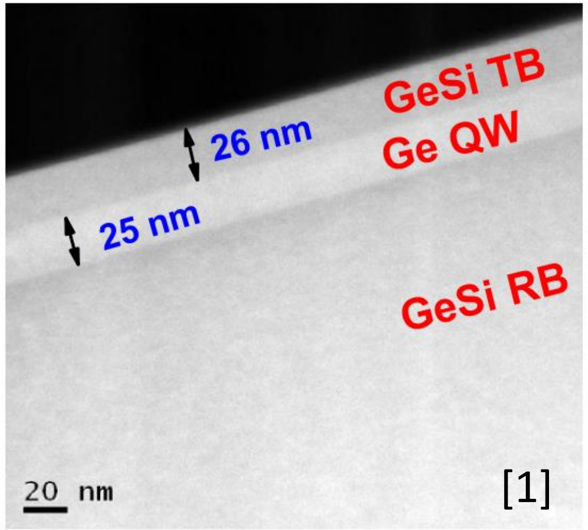

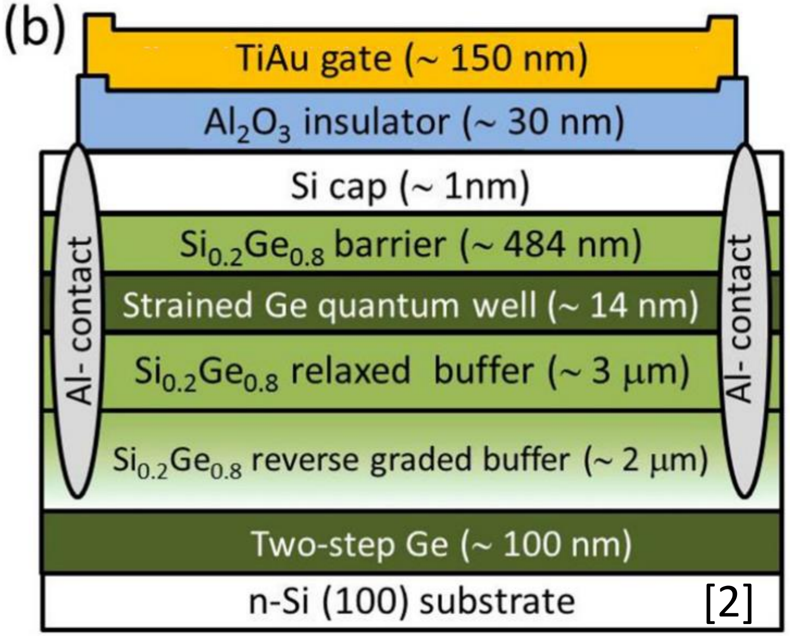

- Here: LT-Ge: 100 nm, HT-Ge: 200 nm, TB: 70 nm
- Q1: 15 % Si, 100 nm Al_2O_3, mobility $\mu > 10^5$ cm²/Vs
- Q2: 28 % Si, 24 nm Al_2O_3 + 1 nm HfO_2, mobility $\mu > 10^5$ cm²/Vs
- Gate design inspired by designs used in Si/SiGe electron systems

[1] Su et al., Phys Rev Mat. 1 044601 (2017)
[2] Laroche et al., APL 108, 233504 (2016)

Hall Bar Measurements I

- Longitudinal and Hall resistance measured in 4He cryostat with variable tempereture
- Mean free path from mobility measurements
  - $\mu \geq 6 \times 10^4$ cm2/Vs
  - High quality samples, low disorder

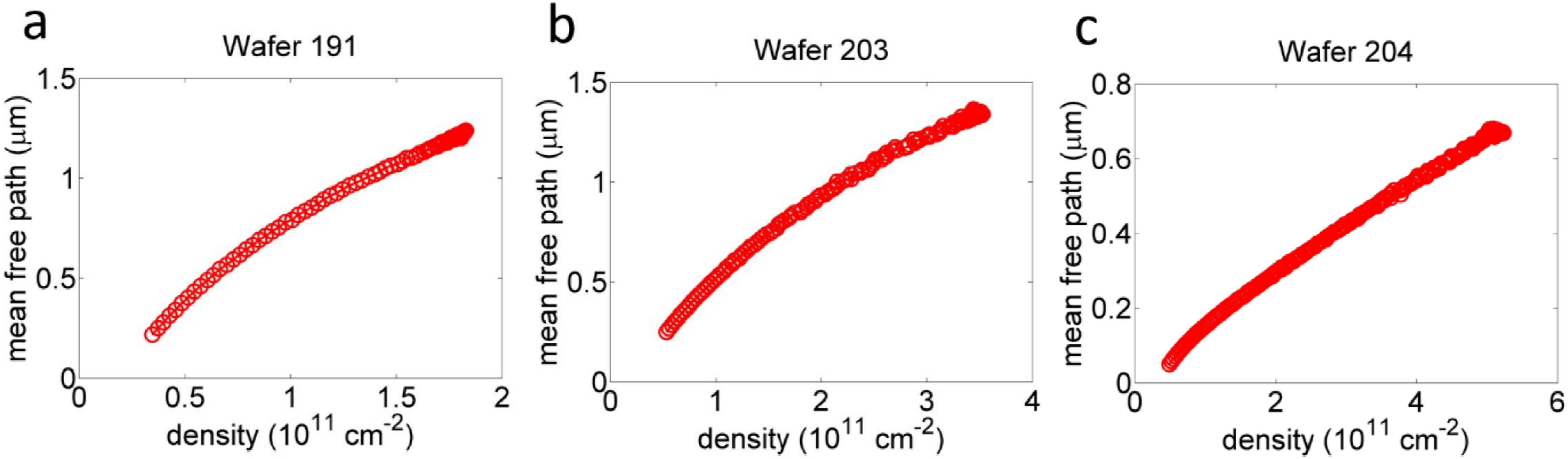

Hall Bar Measurements II

- Magnetoresistance data reveals Shubnikov-de Haas oscillations
  - Shows low disorder of material
  - Inverse proportional to temperature

- Extract amplitudes of even filling factor and trace temperature dependence to extract effective mass at various densities

$$\Delta R_{xx} \propto \frac{2\pi^2 \frac{k_B T}{\Delta E}}{sinh\left[2\pi^2 \frac{k_B T}{\Delta E}\right]}$$

with $\Delta E = heB/2\pi m^*$

- Yields a hole effective mass of $m^* \sim 0.08\ m_0$
  - Note: electron effective mass in GaAs: $m^* \sim 0.067\ m_0$

- Large spacial extent -> enhanced tunnel couplings, facilitation of qubit-qubits interaction, larger lithography

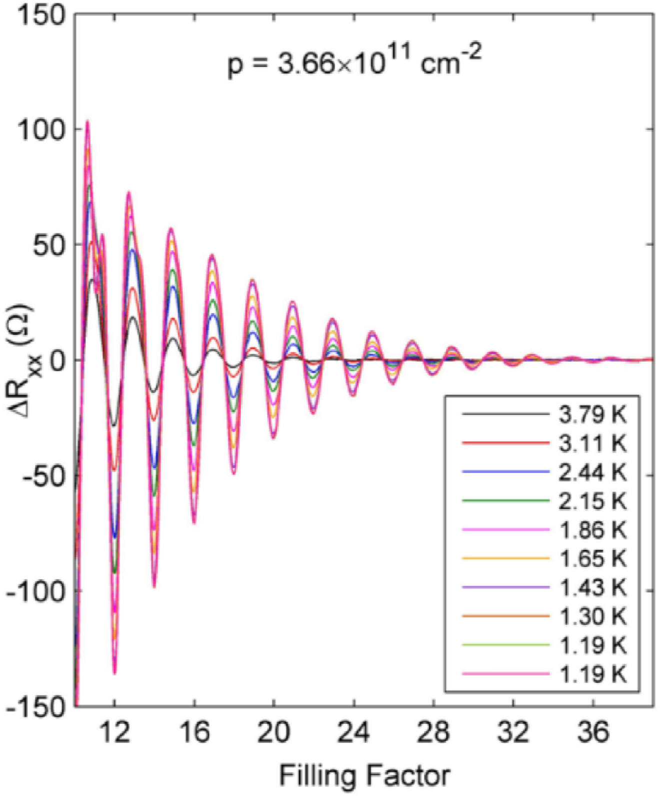

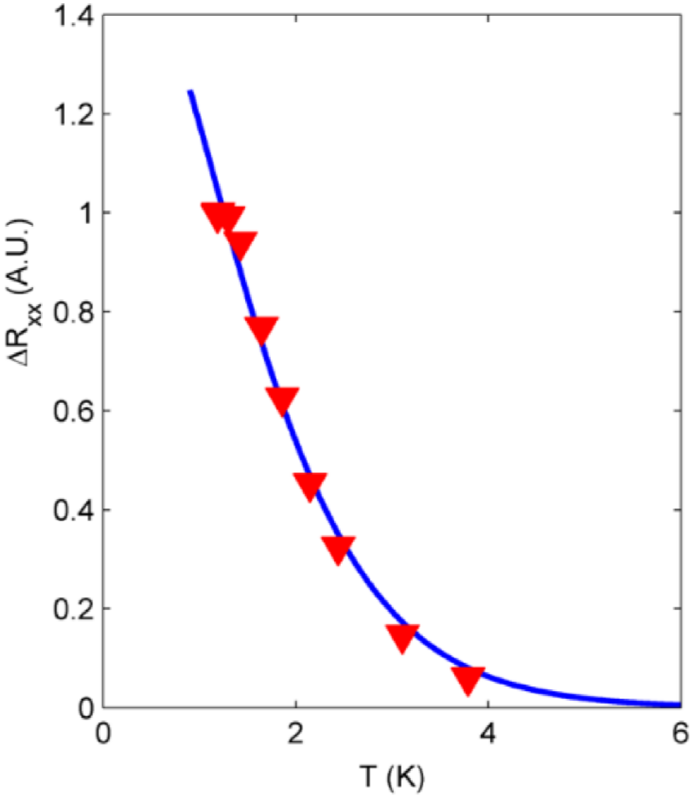

Hall Bar Measurements II

- Magnetoresistance data reveals Shubnikov-de Haas oscillations
  - Shows low disorder of material
  - Inverse proportional to temperature

- Extract amplitudes of even filling factor and trace temperature dependence to extract effective mass at various densities

$$\Delta R_{xx} \propto \frac{2\pi^2 \frac{k_B T}{\Delta E}}{sinh\left[2\pi^2 \frac{k_B T}{\Delta E}\right]}$$

with $\Delta E = heB/2\pi m^*$

- Yields a hole effective mass of $m^* \sim 0.08\ m_0$
  - Note: electron effective mass in GaAs: $m^* \sim 0.067\ m_0$

- Large spacial extent -> enhanced tunnel couplings, facilitation of qubit-qubits interaction, larger lithography

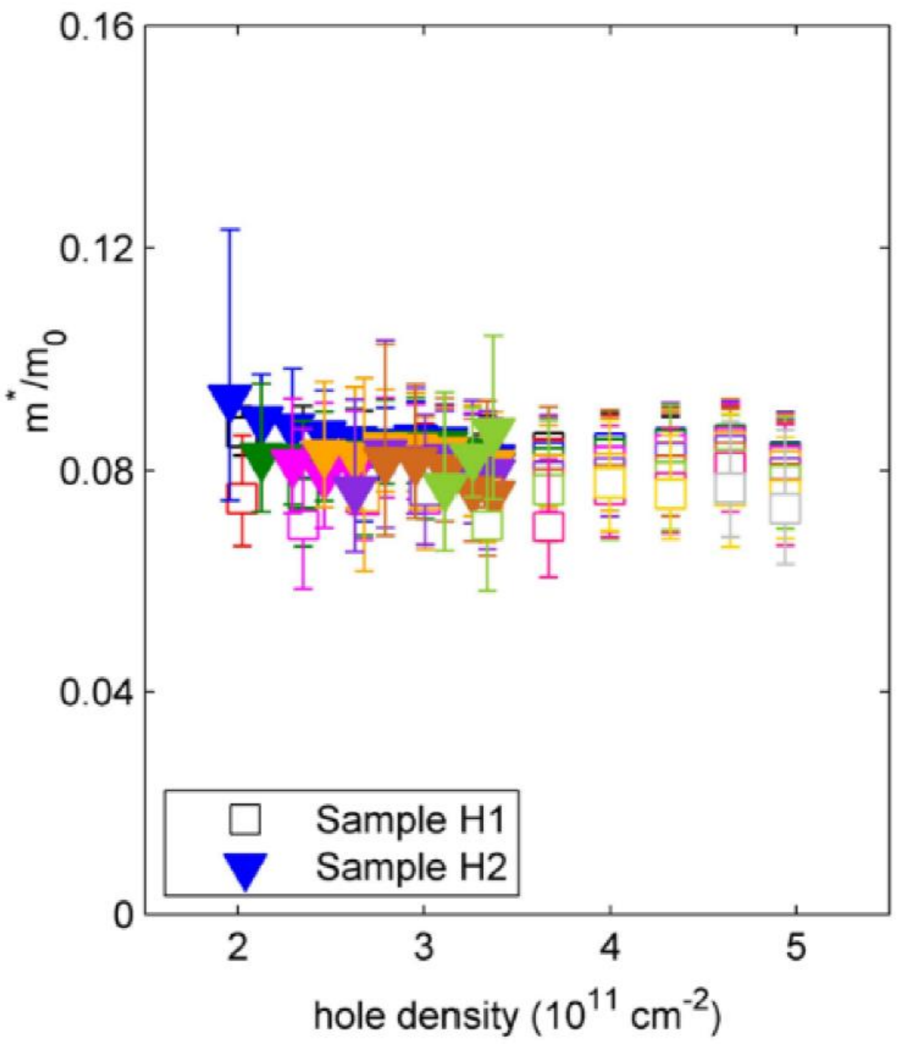

Single Dot I

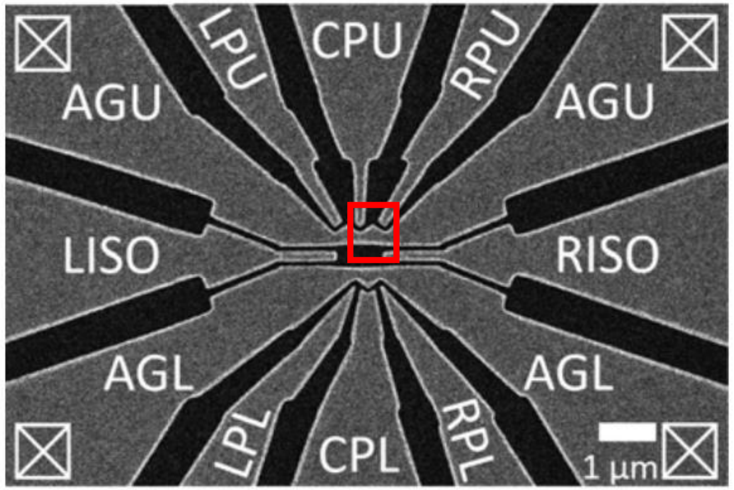

- Measurements performed in dilution refridgerator ($T \sim 30$ mK)
- Accumulation gates: $-0.4\ -\ -1.6$ V; AC bias: 100 μV at 1333 Hz

- CPU fixed, RISO and RPU sweep -> diagonal lines visible
  - Coulomb oscillations corresponding to removal of individual holes

- Broadening due to highly transparent tunnel barriers, not experimental parameters (temperature, voltage bias, …)
  - Excludes possibility to see excited states
  - Consistent with simulations (later slides)

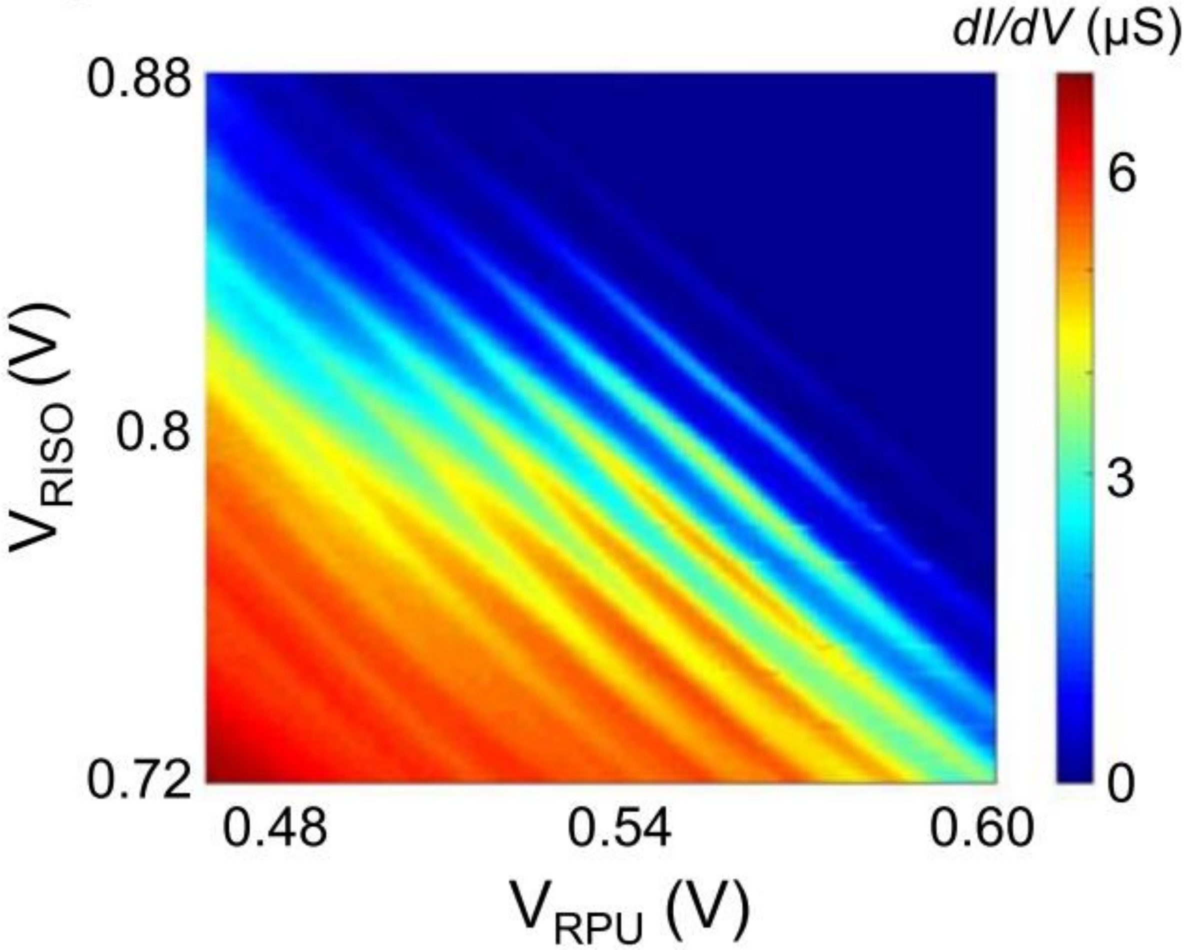

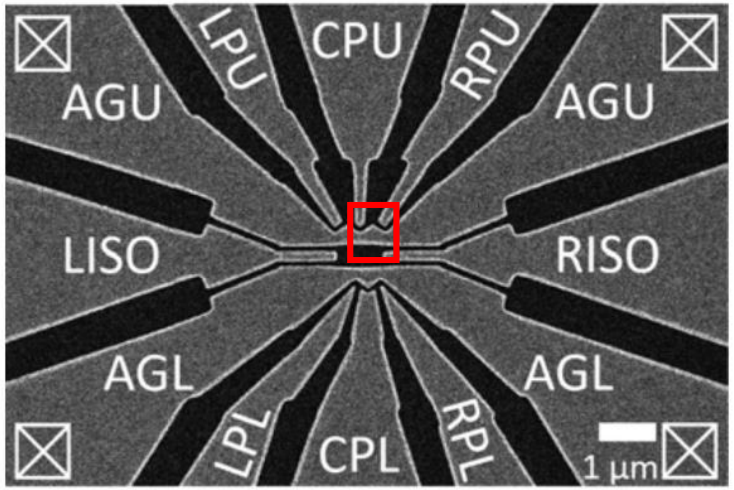

Single Dot II

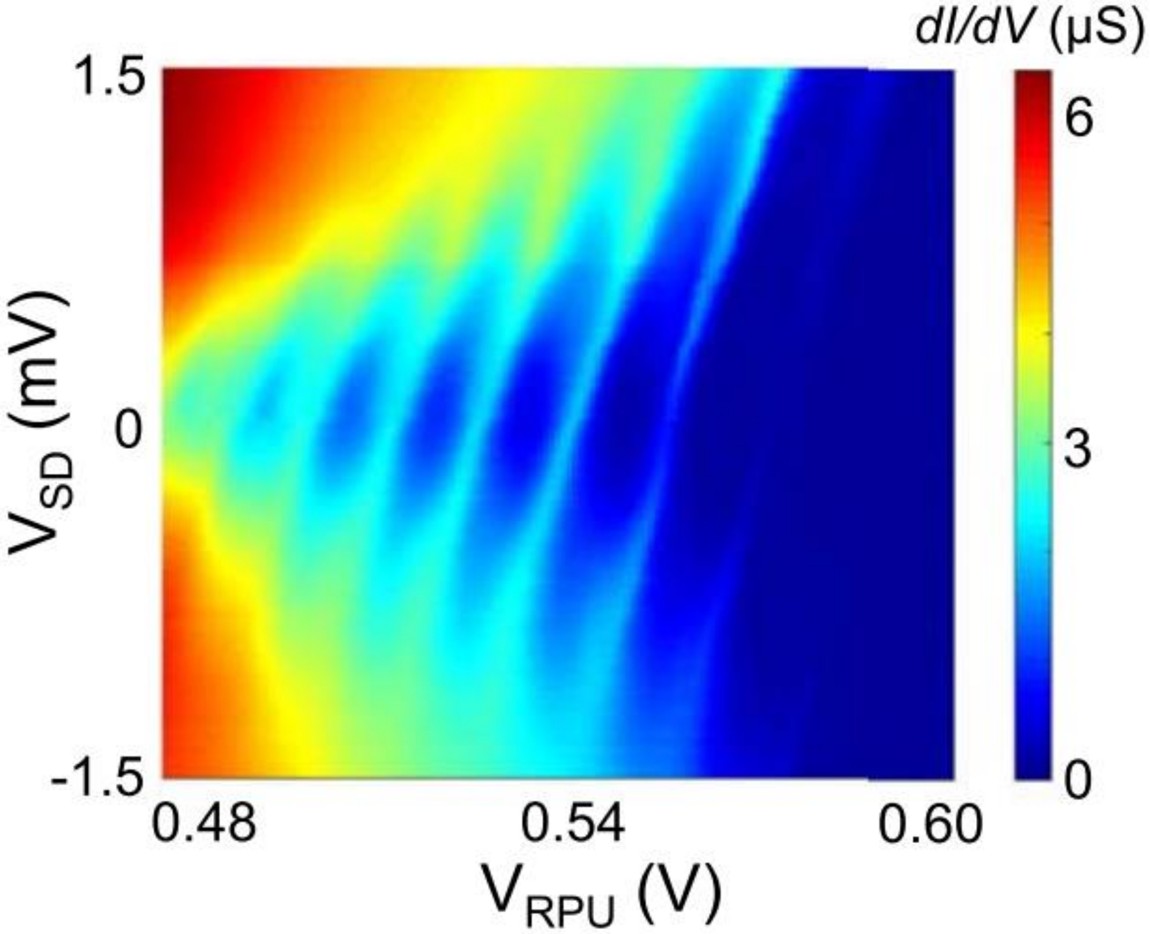

- CPU and RISO fixed, SD and RPU sweep -> Coulomb diamonds
- Diamonds widen -> increasing charging energy -> low occupancy regime
- Capacitance $C_{tot} = \frac{Q}{V} = 92.8$ aF (with V extracted Coulomb oscillation period)
  - Charging energy $E_c = \frac{e^2}{C_{tot}} = 1.7$ meV
  - Consistent with height of Coulomb diamonds

Double Dots

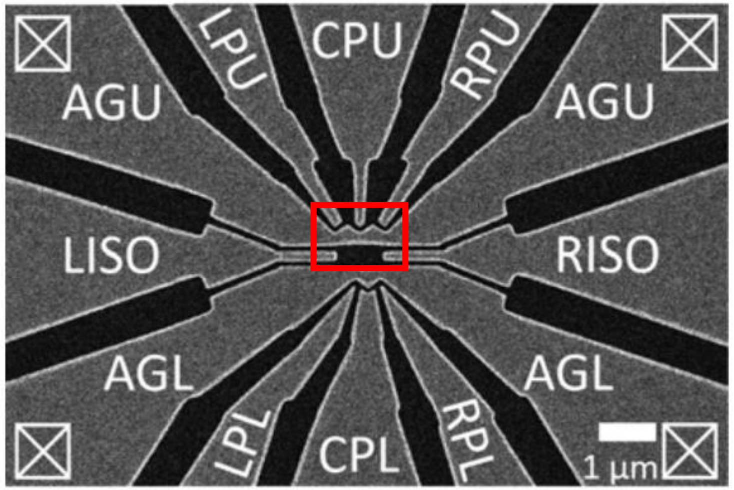

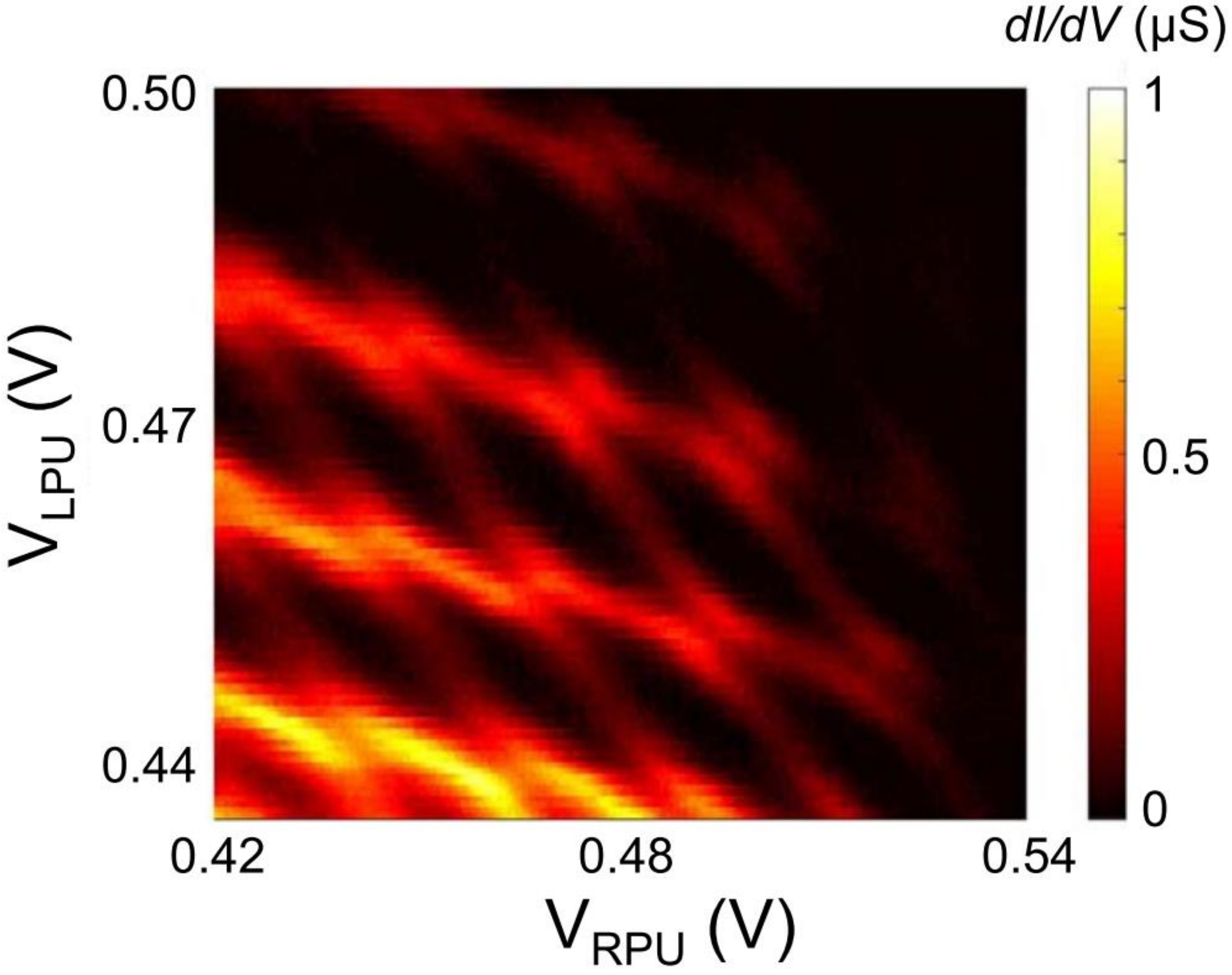

- Device tuneable into double dot regime
  - Visible in stability diagram

- Note: no additional voltage needed on CPU, potential landscape imposed by AGU naturally forms dot

Simulation

- Simulation of device with parameters extracted from SEM images, material stack thickness and dielectric properties
- Gates voltages comparable to actual device (except CPU -> trapped charge in real device)
- Simulation reveals
  - Oblong island -> quantum dot
  - Rapid transition from no charge accumulation to a flooded situation without charge confinement
  - Only few holes possible -> shallow potential
- Further simulations of capacitance -> reasonable agreement with measured capacitances
  - Dot on real device has similar lateral extent

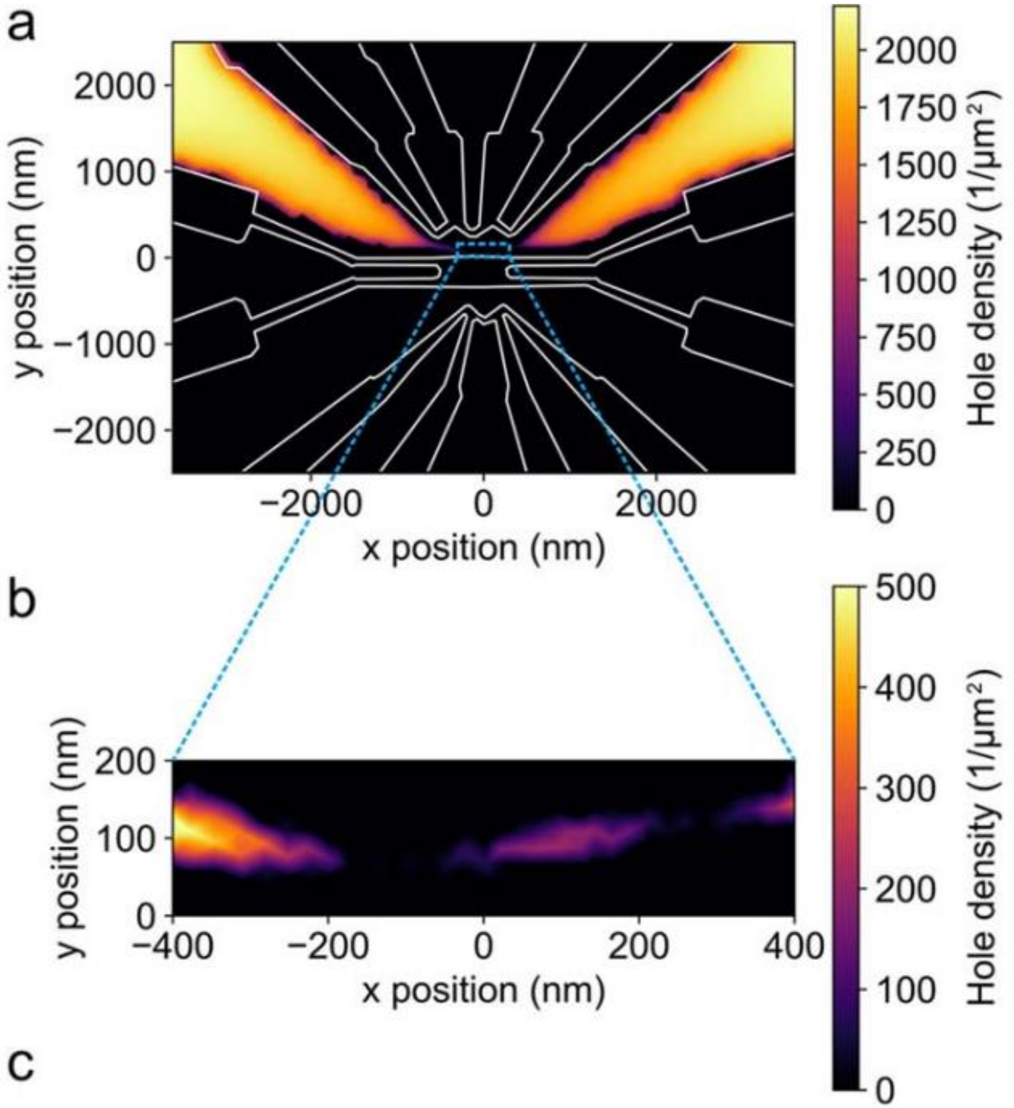

Simulation

- Simulation of device with parameters extracted from SEM images, material stack thickness and dielectric properties

- Gates voltages comparable to actual device (except CPU -> trapped charge in real device)

- Simulation reveals
  - Oblong island -> quantum dot
  - Rapid transition from no charge accumulation to a flooded situation without charge confinement
  - Only few holes possible -> shallow potential

- Further simulations of capacitance -> reasonable agreement with measured capacitances
  - Dot on real device has similar lateral extent

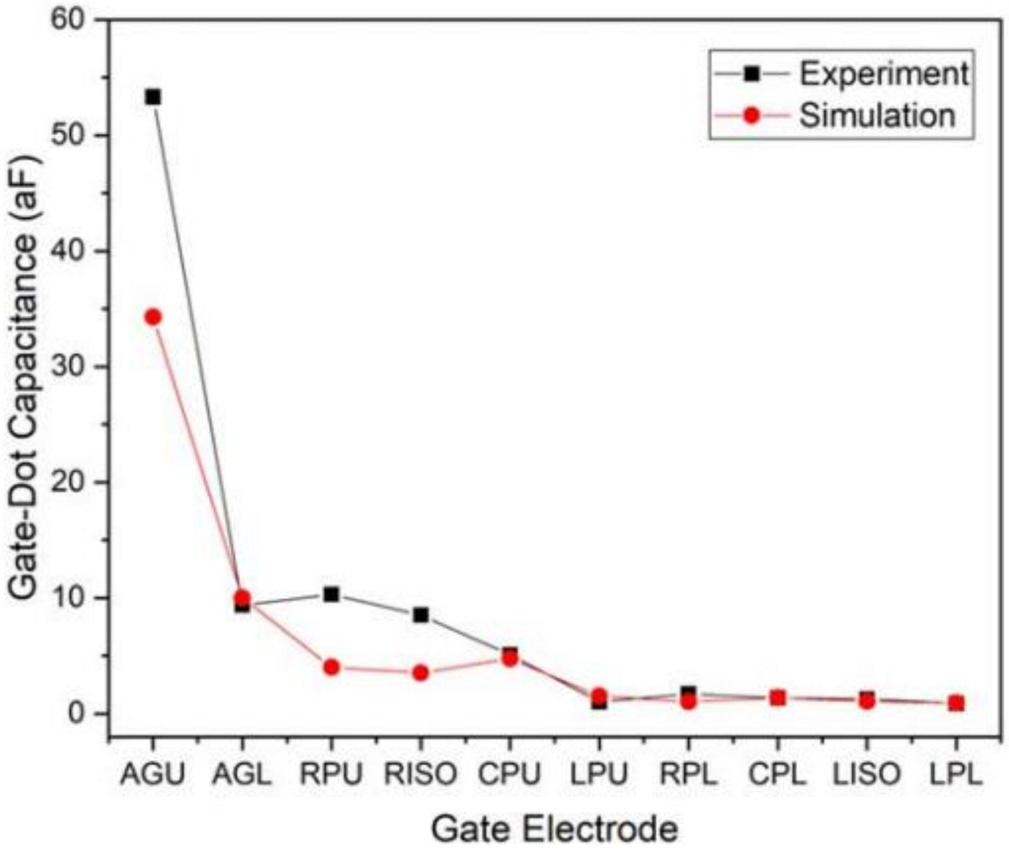

Conclusion

- Demonstration of single and double hole quantum dots in a Ge/SiGe heterostructure with a single gate layer
- Design similar to Si/SiGe systems
    - Allows direct comparison
- Hall measurement reveal hole effective mass of $m^{*} \sim 0.08\ m_0$
    - Similar to GaAs electron effective mass (0.067 m_0)
    - Large wavefunction